Chinese Chemical Letters 36 (2025) 110202

Contents lists available at ScienceDirect

Chinese Chemical Letters

journal homepage: www.elsevier.com/locate/cclet

# New insights into transformation mechanisms for sulfate and chlorine radical-mediated degradation of sulfonamide and fluoroquinolone antibiotics

Jinshuai Zheng[a], Junfeng Niu[b], Crispin Halsall[c], Yadi Guo[a], Peng Zhang[a], Linke Ge[a,c,*]

[a] School of Environmental Science and Engineering, Shaanxi University of Science & Technology, Xi'an 710021, China
[b] College of Environmental Science and Engineering, North China Electric Power University, Beijing 102206, China
[c] Lancaster Environment Centre, Lancaster University, Lancaster LA1 4YQ, United Kingdom

ARTICLE INFO

*Article history:*
Received 4 March 2024
Revised 11 June 2024
Accepted 1 July 2024
Available online 2 July 2024

*Keywords:*
Antibiotics
Dissociation
Degradation kinetics
Reactive species
Transformation pathways
Risks

ABSTRACT

As antibiotic pollutants cannot be incompletely removed by conventional wastewater treatment plants, ultraviolet (UV) based advanced oxidation processes (AOPs) such as UV/persulfate (UV/PS) and UV/chlorine are increasingly concerned for the effective removal of antibiotics from wastewaters. However, the specific mechanisms involving degradation kinetics and transformation mechanisms are not well elucidated. Here we report a detailed examination of $SO_4^{\bullet-}$/$Cl^{\bullet}$-mediated degradation kinetics, products, and toxicities of sulfathiazole (ST), sarafloxacin (SAR), and lomefloxacin (LOM) in the two processes. Both $SO_4^{\bullet-}$/$Cl^{\bullet}$-mediated transformation kinetics were found to be dependent on pH ($P < 0.05$), which was attributed to the disparate reactivities of their individual dissociated forms. Based on competition kinetic experiments and matrix calculations, the cationic forms ($H_2ST^+$, $H_2SAR^+$, and $H_2LOM^+$) were more highly reactive towards $SO_4^{\bullet-}$ in most cases, while the neutral forms (*e.g.*, $HSAR^0$ and $HLOM^0$) reacted the fastest with $Cl^{\bullet}$ for the most of the antibiotics tested. Based on the identification of 31 key intermediates using tandem mass spectrometry, these reactions generated different products, of which the majority still retained the core chemical structure of the parent compounds. The corresponding diverse transformation pathways were proposed, involving S–N breaking, hydroxylation, defluorination, and chlorination reactions. Furthermore, the toxicity changes of their reaction solutions as well as the toxicity of each intermediate were evaluated by the *vibrio fischeri* and ECOSAR model, respectively. Many primary by-products were proven to be more toxic than the parent chemicals, raising the wider issue of extended potency for these compounds with regards to their ecotoxicity. These results have implications for assessing the degradative fate and risk of these chemicals during the AOPs.



Antibiotics, as a class of emerging contaminants, have become an environmental topic of acute concern due to their *pseudo*-persistence and ecological risk in aquatic systems [1-3]. As necessities, antibiotics are widely used in human treatments, animal husbandry, and aquaculture [4-6]. Then, they are mainly released from hospitals and households into wastewater treatment plants (WWTPs) [7,8]. China has attached great importance to eliminate the emerging contaminants. However, most antibiotics cannot be incompletely removed by conventional wastewater treatment processes and are therefore frequently discharged into the aquatic environment [9,10]. Their aqueous ubiquity in surface waters has been reported in many countries, including European countries, the United States, and China [11-13]. Even trace amounts of antibiotics persisting in the aquatic environment can have long-term adverse effects [14]. Antibiotic pollutants are resistant to biodegradation in the environment, but their presence in water systems induces the generation of antibiotic resistant bacteria and poses a threat to ecosystem and human health [15]. Therefore, it is necessary to control such pollutants in wastewater to prevent them from entering the aquatic environment.

Conventional wastewater treatment processes including adsorption, sedimentation, and biodegradation cannot remove antibiotics effectively [16-18]. Ultraviolet (UV) based advanced oxidation processes (AOPs) have been reported to effectively degrade antibiotics [6,19,20]. UV/persulfate (UV/PS) and UV/chlorine have received increasing attention in the degradation of antibiotics in wastewater because of their strong oxidation ability, high efficiency, and lim-

* Corresponding author.
*E-mail address:* gelinke@sust.edu.cn (L. Ge).

https://doi.org/10.1016/j.cclet.2024.110202
1001-8417/

ited secondary pollution [21-23]. Many previous studies have investigated influencing factors of the UV/PS and UV/chlorine processes [24-27], and the pH values of the reaction system were found to significantly affect the degradation efficiency of certain pollutants [28,29]. For instance, although the degradation of sulfachloropyridazine in the UV/PS process at different pH conditions followed *pseudo*-first-order reaction kinetics, the fastest reaction rate appeared at pH 5 [30]. Yang *et al.* [31] observed the fastest degradation of ciprofloxacin (CIP) at pH 7 and pH 5, respectively, in the UV/PS and UV/chlorine processes, and deduced that the phenomena might be attributed to the diverse reactivities of CIP toward reactive species (RS) at different pHs. As the molecular structures contain ionizable groups (*e.g.*, −COOH and $-NH_n$), most antibiotics are ionizable and will undergo acid-base dissociation, exhibiting different dissociated species depending on the pH of the water [32-34]. These dissociated species have been proven to have unique physicochemical properties [34]. As for the UV/PS and UV/chlorine processes, previous studies have found that pH has a significant effect on the degradation of ionizable antibiotics by $SO_4^{\bullet-}$ and $Cl^{\bullet}$, but the specific mechanisms involving the degradation kinetics and transformation products are not well elucidated [23,27,31]. Therefore, it is necessary to clarify the degradation behavior and related mechanisms of antibiotics in different dissociated forms in the two processes.

This study provides a detailed examination of $SO_4^{\bullet-}/Cl^{\bullet}$-mediated degradation of sulfathiazole (ST), sarafloxacin (SAR), and lomefloxacin (LOM) in UV/PS and UV/chlorine systems. ST, SAR, and LOM (purity > 98%) were purchased from J&K Scientific Ltd. (Beijing, China). Their chemical structures and molecular weights are shown in Table S1 (Supporting information). The experiments were carried out using a merry-go-round photochemical reactor with a 500 W mercury lamp (Fig. S1 in Supporting information). In order to avoid direct photolysis of the target compounds, 400 nm cut-off filters were used to adjust the emission spectra of the light source ($\lambda$ > 400 nm). The light intensity at the solutions was 1.83 mW/cm$^2$ at 420 nm. In the competition kinetic experiments, $Na_2S_2O_8$ (40 μmol/L) and NaClO (40 μmol/L) were used to generate $SO_4^{\bullet-}$ and $Cl^{\bullet}$, respectively. The initial concentrations of the antibiotics were set at 5 μmol/L based on the better ratio of the model compounds to the RS [35,36]. The bimolecular reaction rate constants $k_{RS,S}$ ($k_{SO_4^{\bullet-},S}$ and $k_{Cl^{\bullet},S}$) for the three model substances (S) with $SO_4^{\bullet-}$ and $Cl^{\bullet}$ were calculated by Eqs. 1−4 [33,37],

$$k_{RS,S} = \frac{\ln([S]_t/[S]_0)}{\ln([R]_t/[R]_0)} k_{RS,R} \quad (1)$$

$$[^{\bullet}OH]_{SS} = \frac{k_{NB}}{k^{\bullet}_{OH,NB}} \quad (2)$$

$$[Cl^{\bullet}]_{SS} = \frac{k_{BA} - \left[\frac{k^{\bullet}_{OH,BA}}{k^{\bullet}_{OH,NB}}\right] k_{NB}}{k_{Cl^{\bullet},BA}} \quad (3)$$

$$k_{Cl^{\bullet},S} = \frac{k_S - k^{\bullet}_{OH,S}[^{\bullet}OH]_{SS}}{[Cl^{\bullet}]_{SS}} \quad (4)$$

where $k_{RS,R}$ denotes the bimolecular reaction rate constants of the references (R), $k_{SO_4^{\bullet-},BA} = 1.2 \times 10^9$ L mol$^{-1}$ s$^{-1}$, $k_{Cl^{\bullet},BA} = 1.8 \times 10^{10}$ L mol$^{-1}$ s$^{-1}$, $k_{\bullet OH,BA} = 5.9 \times 10^9$ L mol$^{-1}$ s$^{-1}$, $k_{\bullet OH,NB} = 3.9 \times 10^9$ L mol$^{-1}$ s$^{-1}$; $[^{\bullet}OH]_{SS}$ and $[Cl^{\bullet}]_{SS}$ represent the steady-state concentrations of $^{\bullet}OH$ and $Cl^{\bullet}$, respectively. *Vibrio fischeri* was selected to examine the 15-min acute toxicities of the samples during degradation processes according to the international standard method (ISO11348–3–2007). The experimental information is detailed in the supporting information.

In all control experiments without light irradiation or RS photosensitizers, no significant degradation of ST, SAR, and LOM was observed ($P > 0.1$), suggesting that their pyrolysis and hydrolysis were negligible. As shown in Fig. S2 (Supporting information), these model compounds had no light absorption at $\lambda$ > 400 nm, and thus did not undergo direct photolysis (< 2%). When exposed to light irradiation ($\lambda$ > 400 nm), all three compounds disappeared rapidly in the competition kinetic experiments, indicating that they were effectively degraded by $SO_4^{\bullet-}/Cl^{\bullet}$. It can be seen from the degradation curves in Fig. 1 that the apparent reactions of the three individual substances with the RS were conformed to follow *pseudo*-first-order kinetics ($R^2$ > 0.95), depending on the pH. However, the degradation of the substances by the RS ($SO_4^{\bullet-}/Cl^{\bullet}$) was essentially second-order bimolecular reactions. Thus, the calculated values for the bimolecular reaction rate constants ($k_{SO_4^{\bullet-},S}$ and $k_{Cl^{\bullet},S}$) are shown in Table S2 (Supporting information). The $k_{SO_4^{\bullet-},S}$ ranged from $(1.80 \pm 0.05) \times 10^9$ L mol$^{-1}$ s$^{-1}$ for ST (pH 8) to $(8.73 \pm 0.33) \times 10^{10}$ L mol$^{-1}$ s$^{-1}$ for LOM (pH 10), while the $k_{Cl^{\bullet},S}$ ranged from $(3.44 \pm 0.23) \times 10^9$ L mol$^{-1}$ s$^{-1}$ for SAR (pH 10) to $(3.31 \pm 0.002) \times 10^{11}$ L mol$^{-1}$ s$^{-1}$ for LOM (pH 8).

In comparison with the $k_{\bullet OH,S}$ values of ST [33], SAR [38], and LOM [39], which were all in the same order of magnitude ($10^9$), the $k_{SO_4^{\bullet-},S}$ values of ST, SAR, and LOM differed by orders of magnitude ($10^9$−$10^{10}$). Similarly, their $k_{Cl^{\bullet},S}$ values were not in the same order of magnitude. For example, Lei *et al.* [40] determined the $k_{Cl^{\bullet},S}$ values of 88 trace organic contaminants ranged from $3.10 \times 10^9$ L mol$^{-1}$ s$^{-1}$ to $4.08 \times 10^{10}$ L mol$^{-1}$ s$^{-1}$. The significant differences in $k_{SO_4^{\bullet-},S}$ and $k_{Cl^{\bullet},S}$ values among different classes of reactants could be attributed to the higher selectivity of $SO_4^{\bullet-}$ and $Cl^{\bullet}$ [28]. $SO_4^{\bullet-}$ could oxidatively degrade alkanes, alcohols, organic acids, ethers, esters, and most organic compounds containing unsaturated bonds, whereas $Cl^{\bullet}$ was more sensitive to substances containing electron-rich groups such as olefins, phenols, and anilines [40,41].

As shown in Fig. 2a, both $k_{SO_4^{\bullet-},S}$ and $k_{Cl^{\bullet},S}$ of each compound were dependent on pH ($P < 0.05$). As for ST, $k_{SO_4^{\bullet-},ST}$ and $k_{Cl^{\bullet},ST}$ were slightly higher at pH 2 than at pH 5 and 8. However, $k_{SO_4^{\bullet-},S}$ was maximum at pH 5 for SAR reacting with $SO_4^{\bullet-}$, while LOM was the most reactive toward $SO_4^{\bullet-}$ at pH 10. In addition, both the $k_{Cl^{\bullet},S}$ values of SAR and LOM were the greatest when reacting with $Cl^{\bullet}$ at pH 8. The pH dependence of the reactivities in UV/PS and UV/chlorine reactions was caused by Coulomb's force and chemical structures. The coulombic repulsion between reactants under alkaline conditions leads to lower reactivities [42]. Meanwhile, the molecular structures and deprotonation degrees might have impacts on the pH dependence [33,43], indicating that the RS oxidative reactivities of various dissociated forms of these ionizable antibiotics need to be further differentiated.

To quantify the reactivities of each protonated form towards $SO_4^{\bullet-}$ and $Cl^{\bullet}$, the bimolecular reaction rate constants ($k_{SO_4^{\bullet-},i}$, $k_{Cl^{\bullet},i}$) of different dissociated forms (*i*) were obtained by matrix calculations, and the results are shown in Fig. 2b (detailed data listed in Table S3 in Supporting information). The various dissociated forms of the individual antibiotics exhibited different reactivities (from $H_2ST^+$ to $ST^-$; $H_2FQs^+$ to $FQs^-$). For ST, the cationic forms ($H_2ST^+$) were more reactive toward $SO_4^{\bullet-}$ and $Cl^{\bullet}$. The cationic SAR ($H_2SAR^+$) had the highest reactivity towards $SO_4^{\bullet-}$, while the anionic and cationic LOM ($LOM^-$ and $H_2LOM^+$) were more reactive with $SO_4^{\bullet-}$. Interestingly, both SAR and LOM in the neutral forms ($HFQs^0$) showed the fastest reactions when reacting with $Cl^{\bullet}$. Compared with the $SO_4^{\bullet-}$ mediated reaction, the reactivities of FQs toward $Cl^{\bullet}$ varied by 3 orders of magnitude based on the profile (pH 8 or 10).

As the pH increased, the dissociated forms gradually changed (Fig. S3 in Supporting information), which can explain why the ox-

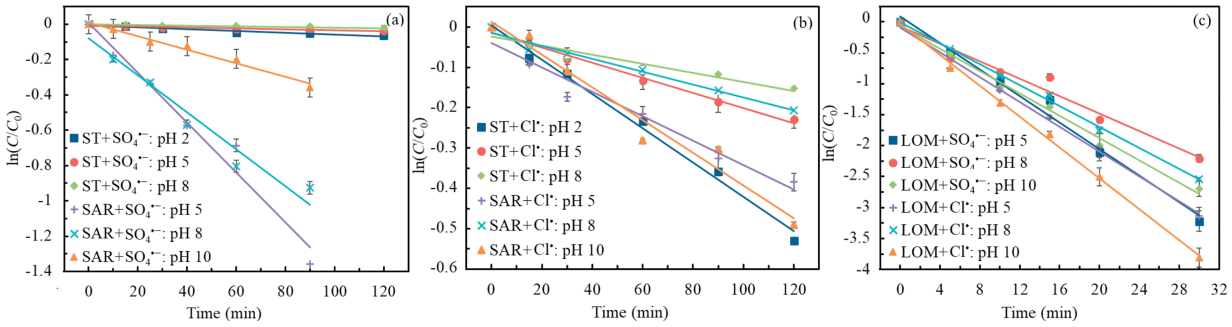


**Fig. 1.** Kinetic profiles for the reactions of sulfathiazole (ST), sarafloxacin (SAR) and lomefloxacin (LOM) with $SO_4^{\bullet-}$/$Cl^{\bullet}$ under different pH conditions.

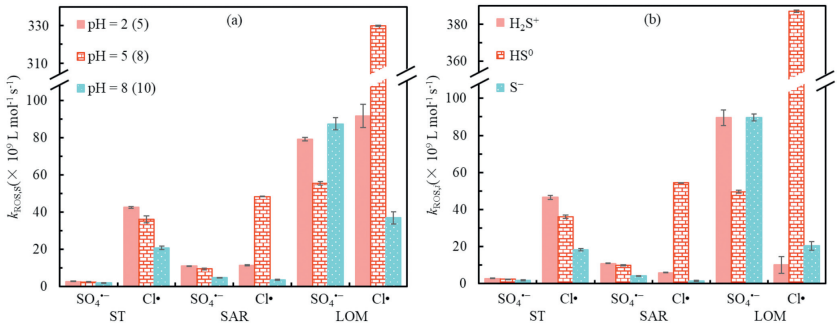


**Fig. 2.** The bimolecular reaction rate constants of ST, SAR, and LOM with $SO_4^{\bullet-}$/$Cl^{\bullet}$. (a) is for different pH conditions, and (b) is for different dissociated forms. S represents the model substances.

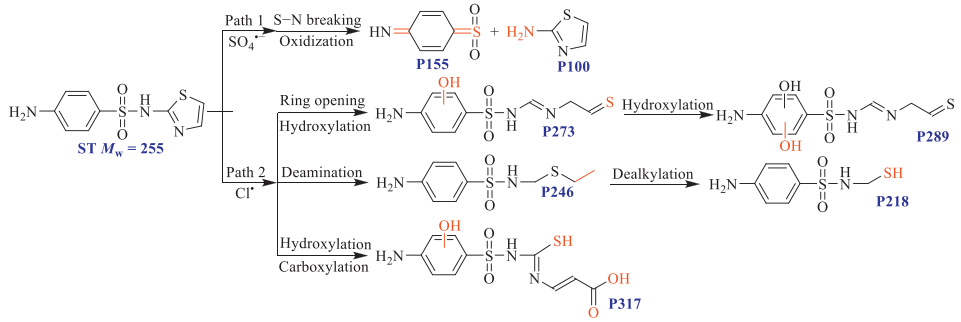


**Fig. 3.** Primary transformation products and pathways of ST during UV/PS and UV/chlorine processes. The products are labeled "P*n*", with *n* standing for the molecular weights.

idation reactivities were significantly related to pH (Fig. 2). Overall, the cationic forms ($H_2ST^+$, $H_2SAR^+$, and $H_2LOM^+$) were more highly reactive towards $SO_4^{\bullet-}$ in most cases, while the neutral forms (*e.g.*, $HSAR^0$ and $HLOM^0$) reacted the fastest with $Cl^{\bullet}$ for most of the antibiotics tested.

Furthermore, we identified 31 significant intermediates generated from $SO_4^{\bullet-}$/$Cl^{\bullet}$-mediated degradation of the three antibiotics in the UV/PS and UV/chlorine processes. The proposed chemical structures and tentative transformation pathways are presented in Figs. 3–5. Table S4 (Supporting information) shows detailed information about these degradation products, including retention times ($t_R$), molecular weights ($M_w$), and MS fragment *m/z*. The total ion chromatograms and MS spectra in positive ionization mode are shown in Figs. S4 and S5 (Supporting information). There are different intermediates and transformation pathways corresponding to the two reactions of the individual antibiotics (Figs. 3–5). As for ST (Fig. 3), the transformation products of the reaction with $SO_4^{\bullet-}$ were simple, mainly because $SO_4^{\bullet-}$ was easy to selectively attack electron-rich groups like anilines [41], resulting in the S–N breaking and the formation of P155 and P100. The products were also detected for the photolysis of ST [44]. In contrast, the primary products in the reaction process of ST with $Cl^{\bullet}$ were abundant, with more reaction pathways involving five-membered heterocyclic ring opening, hydroxylation, and dealkylation. This could be attributed to the diversity of RS ($Cl^{\bullet}$ and $^{\bullet}OH$) in the UV/chlorine process [45]. The $^{\bullet}OH$ preferred to experience multi-site oxidation with phenyl hydroxylation and heterocyclic cleavage [33], while $Cl^{\bullet}$ was easy to attack single bonds and amino groups [21,40]. Therefore, the five-membered heterocycles in the ST structure were easily cleaved.

For SAR (Fig. 4), the same transformation products, P359 and P383, were observed in both UV/PS and UV/chlorine processes. This is mainly due to the susceptibility of SAR's piperazine ring and –F group to be attacked by the RS, resulting in ring opening and defluorination reactions [46]. Meanwhile, there were different degradation products (P232, P351, and P381, *etc.*) generated during the two processes because of the different oxidation capacities and attack sites of $SO_4^{\bullet-}$ and $Cl^{\bullet}$. Based on the transformation products of SAR, then primary reaction pathways were proposed. These included: defluorination; hydroxylation; and piperazinyl cleavage. Importantly, SAR underwent chlorination during the UV/chlorine process, indicating the participation of $Cl^{\bullet}$ in the reaction. The chlo-

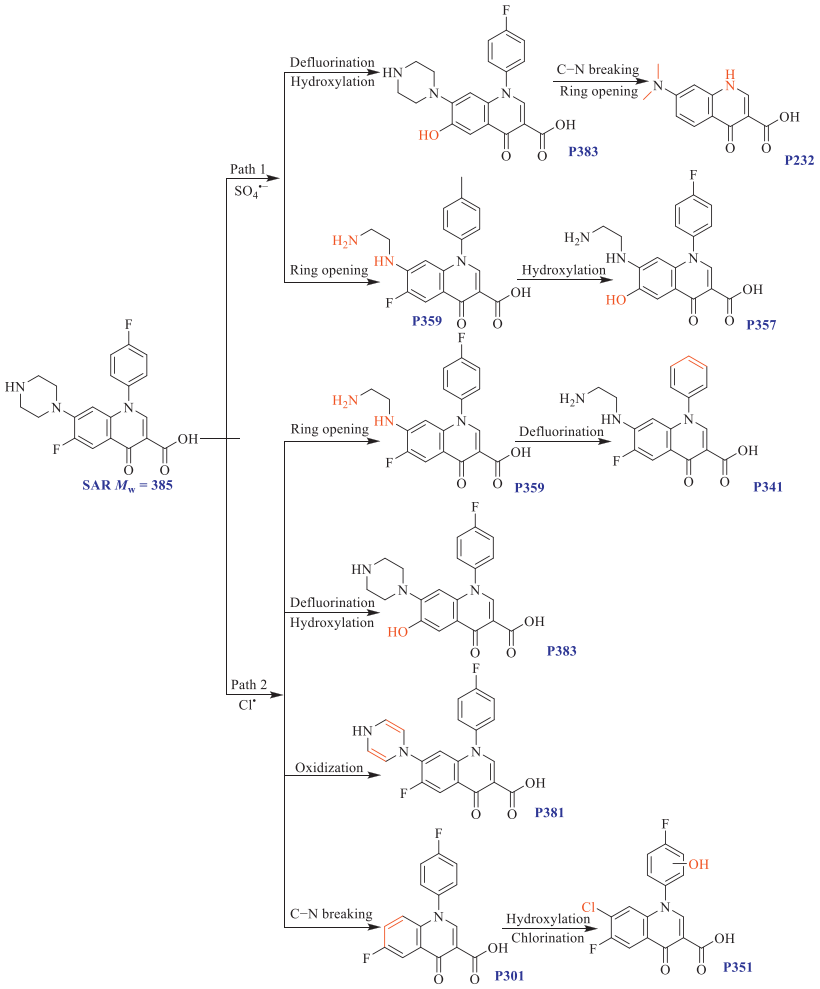


**Fig. 4.** Products and primary pathways of SAR reacting with $SO_4^{\bullet-}$/$Cl^{\bullet}$.

rinated product (P351) is of concern due to its complex biological effects [47-49]. Compared with SAR, the more degradation products (P273, P331, and P349) of LOM (Fig. 5) were similar for UV/PS and UV/chlorine processes, mainly because LOM has more alkane structures and is susceptible to attack by $SO_4^{\bullet-}$ and $Cl^{\bullet}$ [41]. Based on these transformation products, the proposed primary pathways of LOM are defluorination, piperazinyl ring opening, hydroxylation, *etc.*

The toxicity of the 3 target antibiotics during the $SO_4^{\bullet-}$/$Cl^{\bullet}$ mediated degradation processes was assayed, for which the results are shown in Fig. 6. There were certain similarities and differences in the toxicity changes for the individual antibiotics towards the two RS. For ST, the toxicities of both reaction systems first increased, and then decreased with time, implying the generation of some more toxic intermediates than the parent compound. However, toxicities for the $Cl^{\bullet}$ mediated reaction solution of ST were more enhanced at the initial period ($0-t_{1/2}$) of degradation, which can be attributed to the abundant intermediates that contain the basic parent structure (Fig. 3).

As for SAR and LOM, their toxicity profiles were diverse between the two reaction systems (Fig. 6). The toxicities observed during the reaction of SAR with $SO_4^{\bullet-}$ showed an overall decreasing trend with time, while the toxicities were initially reduced and then enhanced during the reaction between SAR and $Cl^{\bullet}$. Unlike SAR, the toxicity trends of LOM during the reaction with $SO_4^{\bullet-}$ and $Cl^{\bullet}$ were similar, which may be due to the formation of similar transformation products (Fig. 5).

The observed toxicity profile was related to the formation and accumulation of transformation products, of which some would be more toxic and others less toxic than the parent compounds. The toxicities of these individual intermediates were assessed using ECOSAR v2.0 software, with their 96 h $LC_{50}$ (fish), 48 h $LC_{50}$ (daphnia), and 96 h $EC_{50}$ values (green algae) shown in Table S5 (Supporting information). It can be found that ST, SAR, and LOM all generated intermediates with higher toxicities than the parents during the degradation processes, such as the transformation products **P100**, **P218**, and **P246** for ST, **P301**, **P351**, **P357**, and **P383** for SAR, as well as **P275** and **P289** for LOM. This suggested that the toxicities of the reaction systems would persist in these initial intermediates, showing good consistence with the results of the *vibrio fischeri* toxicity experiments. Therefore, the ecological risks of the treated antibiotic wastewaters by the UV/PS and UV/chlorine processes need to be considered before treated-wastewater release into the aquatic environment.

In summary, this study provides new insights into the $SO_4^{\bullet-}$/$Cl^{\bullet}$-mediated degradation kinetics, products, toxicities, and related mechanisms of the three representative antibiotics in UV/PS and UV/chlorine processes. The transformation kinetics were found to be dependent on pH ($P < 0.05$), which was attributable to the disparate reactivities of their individual dissociated forms when reacting with RS (*e.g.*, $SO_4^{\bullet-}$ and $Cl^{\bullet}$). These reactions generated different products, and demonstrated diverse transformation pathways, involving S–N cleavage, hydroxylation, defluorination, and chlorination reactions. This has implications when assess-

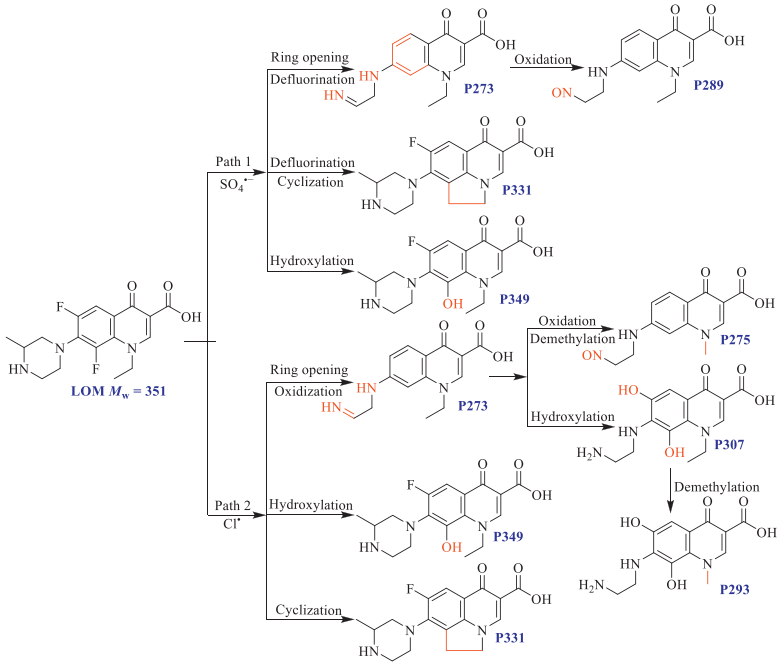


**Fig. 5.** Transformation products and primary pathways of LOM during UV/PS and UV/chlorine processes.

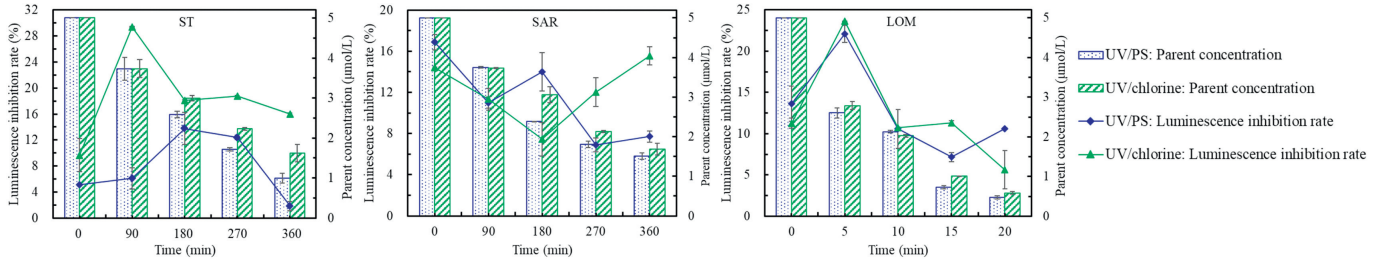


**Fig. 6.** Concentration changes and solution luminescence inhibition rates of ST, SAR, and LOM during UV/PS and UV/chlorine processes.

ing the degradative fate of these chemicals during the AOPs that are increasingly used in tertiary wastewater treatment processes.

Furthermore, we found that many primary by-products exhibited similar structures to the parent compounds and revealed the toxicity profiles of ST, SAR, and LOM reaction systems before and after degradation. The toxicity responses were dependent on the major intermediates and primary pathways. Many intermediates were proven to be more toxic than their individual parents, raising the wider issue of extended potency for these compounds with regards to their ecotoxicity. These results provide novel knowledge for understanding the UV-based AOPs to treat wastewater containing antibiotics.

## Declaration of competing interest

The authors declare that they have no known competing financial interests or personal relationships that could have appeared to influence the work reported in this paper.

## CRediT authorship contribution statement

**Jinshuai Zheng:** Writing – review & editing, Writing – original draft, Methodology, Data curation, Conceptualization. **Junfeng Niu:** Writing – review & editing. **Crispin Halsall:** Writing – review & editing. **Yadi Guo:** Writing – review & editing. **Peng Zhang:** Writing – review & editing, Supervision. **Linke Ge:** Writing – review & editing, Supervision, Funding acquisition, Conceptualization.

## Acknowledgments

This work was supported by the Key Research and Development Program of Shaanxi Province (No. 2024SF-YBXM-567), the National Natural Science Foundation of China (Nos. 21976045, 22076112), and the China Scholarship Council (CSC) Scholarship (No. 202308610123).

## Supplementary materials

Supplementary material associated with this article can be found, in the online version, at doi:10.1016/j.cclet.2024.110202.

## References

[1] E. Brillas, Sci. Total Environ. 819 (2022) 153102.
[2] K. Brooks, J. Eze, O. Onalenna, T.O. Rahube, J. Hazard. Mater. Adv. 9 (2023) 100232.
[3] H. Malik, R. Singh, S. Kaur, et al., J. Infect. Public Health 16 (2023) 172–182.
[4] J. Ren, H. Shi, J. Liu, et al., J. Environ. Manage. 335 (2023) 117546.
[5] X. Wang, J. Jing, M. Zhou, R. Dewil, Chin. Chem. Lett. 34 (2023) 107621.
[6] R. Guo, Y. Chen, B. Liu, et al., Chin. Chem. Lett. 33 (2022) 3809–3817.
[7] F. Yan, L. An, X. Xu, W. Du, R. Dai, Sci. Total Environ. 906 (2024) 167737.
[8] C. Zhang, Y. Chen, S. Chen, et al., Ecotoxicol. Environ. Saf. 255 (2023) 114817.
[9] J. Wang, R. Zhuan, L. Chu, Sci. Total Environ. 646 (2019) 1385–1397.
[10] Y. Pan, Y. Zhang, M. Zhou, J. Cai, Y. Tian, Water Res. 153 (2019) 144–159.
[11] C.E. Givens, D.W. Kolpin, L.E. Hubbard, et al., Sci. Total Environ. 904 (2023) 166753.
[12] D. Han, Q. Hou, J. Song, et al., Environ. Res. 235 (2023) 116653.
[13] U. Szymańska, M. Wiergowski, I. Sołtyszewski, et al., Microchem. J. 147 (2019) 729–740.

[14] G. Liu, H. Zheng, J. Lu, Trends Environ, Anal. Chem. 16 (2017) 16–23.
[15] N. Guo, Y. Wang, L. Yan, et al., Water Res. 117 (2017) 95–101.
[16] J. Dutta, A.A. Mala, Water Sci. Technol. 82 (2020) 401–426.
[17] A.C. Reis, B.A. Kolvenbach, O.C. Nunes, P.F. Corvini, New Biotechnol 54 (2020) 34–51.
[18] D. Zhi, D. Yang, Y. Zheng, et al., J. Environ. Manage. 251 (2019) 109598.
[19] Z. Li, J. Wang, J. Chang, B. Fu, H. Wang, Sci. Total Environ. 857 (2022) 159172.
[20] J. Liu, H. He, Z. Shen, H.H. Wang, W. Li, J. Hazard. Mater. 429 (2022) 128398.
[21] N. Li, J. Ye, H. Dai, et al., Water Res. 235 (2023) 119926.
[22] Z. Li, L. Wang, Y. Liu, et al., Water Res. 195 (2021) 116973.
[23] Y. Zhang, L. Li, Z. Pan, et al., Chem. Eng. J. 379 (2020) 122354.
[24] E. Bazrafshan, P. Tavassoli, A.A. Zarei, Water Sci. Technol. 2017 (2018) 126–133.
[25] N. Huang, W. Wang, Z. Xu, Q. Wu, H. Hu, J. Environ. Manage. 237 (2019) 180–186.
[26] M.Y. Kilic, W.H. Abdelraheem, X. He, K. Kestioglu, D.D. Dionysiou, J. Hazard. Mater. 367 (2019) 734–742.
[27] Y. Zhang, J. Zhang, Y. Xiao, V.W.C. Chang, T.T. Lim, Chem. Eng. J. 302 (2016) 526–534.
[28] M. Xu, J. Deng, A. Cai, et al., Chem. Eng. J. 413 (2021) 127533.
[29] Z. Xu, C. Shan, B. Xie, Y. Liu, B. Pan, Appl. Catal. B 200 (2017) 439–447.
[30] J. Dan, Q. Wang, K. Mu, et al., Environ. Sci. Water Res. Technol. 6 (2020) 2510–2520.
[31] H. Yang, Y. Li, Y. Chen, G. Ye, X. Sun, Water Environ. Res. 91 (2019) 1576–1588.
[32] L. Ge, Q. Dong, C. Halsall, et al., Environ. Sci. Pollut. Res. 25 (2018) 15726–15732.
[33] L. Ge, P. Zhang, C. Halsall, et al., Water Res. 149 (2019) 243–250.
[34] X. Wei, J. Chen, Q. Xie, et al., Environ. Sci. Technol. 47 (2013) 4284–4290.
[35] X. Liu, Y. Liu, S. Lu, et al., Chem. Eng. J. 385 (2020) 123987.
[36] Z. Wu, S. Gong, J. Liu, J. Shi, H. Deng, J. Water Process Eng. 58 (2024) 104870.
[37] J. Fang, Y. Fu, C. Shang, Environ. Sci. Technol. 48 (2014) 1859–1868.
[38] L. Ge, G. Na, S. Zhang, et al., Sci. Total Environ. 527 (2015) 12–17.
[39] X. Luo, X. Wei, J. Chen, et al., Water Res. 166 (2019) 115083.
[40] Y. Lei, S. Cheng, N. Luo, X. Yang, T. An, Environ. Sci. Technol. 53 (2019) 11170–11182.
[41] X. Li, J. Shen, H. Cao, et al., Chem. Eng. J. 474 (2023) 146256.
[42] X. Tong, S. Wang, L. Wang, Chemosphere 256 (2020) 126997.
[43] T. Mill, Chemosphere 38 (1999) 1379–1390.
[44] A.L. Boreen, W.A. Arnold, K. McNeill, Environ. Sci. Technol. 38 (2004) 3933–3940.
[45] T.K. Kim, T. Kim, Y. Cha, K.D. Zoh, Water Res. 185 (2020) 116159.
[46] N. Li, R. Li, X. Duan, et al., Environ. Sci. Technol. 55 (2021) 16163–16174.
[47] S. Kali, M. Khan, M.S. Ghaffar, et al., Environ. Pollut. 281 (2021) 116950.
[48] B.T. Oba, X. Zheng, M.A. Aborisade, et al., Environ. Pollut. 291 (2021) 118239.
[49] A. Riu, A. le Maire, M. Grimaldi, et al., Toxicol. Sci. 122 (2011) 372–382.